AMERICAN JOURNAL OF PHYSIOLOGY
ENDOCRINOLOGY AND METABOLISM

Am J Physiol Endocrinol Metab 320: E967–E975, 2021.
First published March 22, 2021; doi:10.1152/ajpendo.00565.2020

RESEARCH ARTICLE

Osteocyte- and late osteoblast-derived NOTUM reduces cortical bone mass in mice

Karin H. Nilsson,[1] Petra Henning,[1] Maha El Shahawy,[1,4] Jianyao Wu,[1] Antti Koskela,[2] Juha Tuukkanen,[2] Christine Perret,[3] Ulf H. Lerner,[1] Claes Ohlsson,[1] and Sofia Movérare-Skrtic[1]

[1]*Department of Internal Medicine and Clinical Nutrition, Institute of Medicine, Centre for Bone and Arthritis Research at the Sahlgrenska Academy, University of Gothenburg, Gothenburg, Sweden;* [2]*Department of Anatomy and Cell Biology, Faculty of Medicine, Institute of Cancer Research and Translational Medicine, University of Oulu, Oulu, Finland;* [3]*Université de Paris, Institut Cochin, INSERM, CNRS, Paris, France; and* [4]*Department of Oral Biology, Minia University, Minia, Egypt*

Abstract

Osteoporosis is a common skeletal disease, with increased risk of fractures. Currently available osteoporosis treatments reduce the risk of vertebral fractures, mainly dependent on trabecular bone, whereas the effect on nonvertebral fractures, mainly dependent on cortical bone, is less pronounced. WNT signaling is a crucial regulator of bone homeostasis, and the activity of WNTs is inhibited by NOTUM, a secreted WNT lipase. We previously demonstrated that conditional inactivation of NOTUM in all osteoblast lineage cells increases the cortical but not the trabecular bone mass. The aim of the present study was to determine if NOTUM increasing cortical bone is derived from osteoblast precursors/early osteoblasts or from osteocytes/late osteoblasts. First, we demonstrated *Notum* mRNA expression in *Dmp1*-expressing osteocytes and late osteoblasts in cortical bone using in situ hybridization. We then developed a mouse model with inactivation of NOTUM in *Dmp1*-expressing osteocytes and late osteoblasts (*Dmp1-creNotum*$^{flox/flox}$ mice). We observed that the *Dmp1-creNotum*$^{flox/flox}$ mice displayed a substantial reduction of *Notum* mRNA in cortical bone, resulting in increased cortical bone mass and decreased cortical porosity in femur but no change in trabecular bone volume fraction in femur or in the lumbar vertebrae L5 in *Dmp1-creNotum*$^{flox/flox}$ mice as compared with control mice. In conclusion, osteocytes and late osteoblasts are the principal source of NOTUM in cortical bone, and NOTUM derived from osteocytes/late osteoblasts reduces cortical bone mass. These findings demonstrate that inhibition of osteocyte/late osteoblast-derived NOTUM might be an interesting pharmacological target to increase cortical bone mass and reduce nonvertebral fracture risk.

NEW & NOTEWORTHY NOTUM produced by osteoblasts is known to regulate cortical bone mass. Our new findings show that NOTUM specifically derived by *DMP1*-expressing osteocytes and late osteoblasts regulates cortical bone mass and not trabecular bone mass.

cortical bone; NOTUM; osteocytes

INTRODUCTION

Osteoporosis is a common skeletal disease, leading to a reduction in bone density and quality and an increased fracture risk. One in two elderly women and one in four elderly men will at some point suffer from an osteoporotic fracture and the prevention of fractures is an important public health goal (1, 2).

Approximately 80% of the human skeleton is comprised of cortical bone, and the cortical bone mass and quality are crucial for the overall bone strength. Most of the osteoporotic fractures occur at nonvertebral bone sites, mainly dependent on cortical bone (3, 4). Currently used antiresorptive drugs substantially reduce the risk of vertebral fractures, mainly dependent on decreased trabecular bone mass, whereas the effect on nonvertebral fractures is less pronounced, suggesting that trabecular and cortical bone might respond differently to signals involved in the regulation of skeletal homeostasis (5). Although cortical bone mass and quality are major determinants of bone strength and fracture risk in humans (1, 6, 7), only a limited number of studies have focused on the cellular and molecular mechanisms specifically regulating cortical bone mass (1, 6, 7).

WNT signaling is a crucial regulator of bone homeostasis, and WNT ligands are known to affect bone mass by targeting the trabecular and/or cortical bone compartments (5, 8). WNT16 is the major known cortical bone-specific WNT (5), while WNT10b protects against age-dependent trabecular bone loss (9, 10). The activity of WNTs is inhibited by NOTUM, a secreted WNT lipase highly expressed

Correspondence: K. H. Nilsson (karin.nilsson.2@gu.se).
Submitted 11 November 2020 / Revised 24 February 2021 / Accepted 16 March 2021

by the osteoblast lineage cells in cortical bone (11–14). NOTUM acts as a WNT inhibitor by deacetylating WNT proteins, making them unable to bind to their receptor Frizzled (12).

We have previously reported that osteoblast-derived NOTUM reduces cortical bone mass in mice and that the *NOTUM* locus is associated with bone mineral density in humans (11, 13). The specific effect of NOTUM on cortical bone was demonstrated by mice with heterozygous global lifelong deletion of *Notum*, mice with lifelong inactivation of *Notum* in both early and late osteoblast-lineage cells (*Runx2-cre* mouse model), and mice with a globally induced inactivation of *Notum* in adulthood (*CAGG-cre-ER* mouse model), all of which experienced increased cortical bone mass and cortical bone quality with no effect on the trabecular bone mass (11, 13). In the mouse model with an inducible inactivation of *Notum* in adulthood, we observed that the increased cortical bone mass was caused by a rapid increase in cortical bone formation. In contrast, for the *Notum* inactivated mouse models with increased cortical bone mass as a result of lifelong inactivation of *Notum*, adult bone turnover was essentially unchanged as a new steady state had been reached (13).

It is unknown if NOTUM with an impact on cortical bone is derived from osteoblast precursors/early osteoblasts or from osteocytes/late osteoblasts. In this study, we hypothesized that osteocytes/late osteoblasts are the principal source of NOTUM with an impact on cortical bone. We, therefore, determined *Notum* expression in *Dmp1*-expressing osteocytes and late osteoblasts, and we evaluated the skeletal phenotype of a novel mouse model with *Notum* inactivated specifically in *Dmp1*-expressing osteocytes and late osteoblasts.

MATERIALS AND METHODS

Generation of *Dmp1-creNotum$^{flox/flox}$* Mice

To generate mice with a specific inactivation of *Notum* in dentin matrix protein 1 (*Dmp1*)-expressing cells, mice with two *LoxP* sites flanking exons 2–8 of the *Notum* allele (*Notum$^{flox/flox}$*) (15) were bred with the previously described *Dmp1-cre* mice (16). The *Notum$^{flox/flox}$* mice were on C57BL/6J background whereas the *Dmp1-cre* mice were on C57BL/6N background. The offspring expressing both *Dmp1-cre* and two *LoxP* sites, hereafter called *Dmp1-creNotum$^{flox/flox}$* mice, were lacking *Notum* in *Dmp1*-expressing cells, i.e., late osteoblasts and osteocytes. As littermate controls, *Notum$^{flox/flox}$* mice were used.

Genotyping of the *Notum$^{flox/flox}$* mice have been previously described (13). Briefly, the *Notum^{flox}* allele was detected using multiplex real-time PCR analysis (StepOnePlus Real-Time PCR System, Thermo Fischer Scientific, Waltham, MA). The following primers and carboxyfluorescein (FAM)-labeled probe were used to detect the *Notum^{flox}* allele: forward (5′-CCATGATCCTGTGCCTTTCT-3′), reverse (5′-CGACGCGTGAAGTTCCTATT-3′), and probe (5′-GGCCGCGAAGTTCCTATACT-3′), and the following primers and VIC-labeled probe were used to detect the *Notum^{+}* allele: forward (5′-CCATGATCCTGTGCCTTTCT-3′), reverse (5′-AGTGGCATCGGAGACAAATC-3′), and probe (5′-TTGGCAGCCCCAAAATATAG-3′). Genotyping for detecting the presence of the *Dmp1-cre* was done with the following primers: Cre forward (5′-GTTCGCAAGAACCTGATGGACA-3′), Cre reverse (5′-CTAGAGCCTGTTTTGCACGTTC-3′), control primer forward (5′-ACCATGGAGATTAACCCTGACTACG-3′), and control primer reverse (5′-GTGTGTCTGGAAGGTAGCGGTC-3′).

Male and female mice included in the experiment were euthanized at 20 wk of age. All animal experiments included in this study were approved by the Ethics Committee in Gothenburg, and the care of the animals was according to their guidelines. The mice were housed in a standard animal housing facility with a 12-h dark-light period. Food and water were available ad libitum. Before termination, the mice were given an intraperitoneal injection with Ketalar (Pfizer, New York, NY) and Dexdomitor (Orion Pharma, Esbo, Finland) before they were bled and euthanized with cervical dislocation.

Assessment of Bone Parameters

Dual-energy X-ray absorptiometry.

Total body bone mineral density (BMD) was assessed using the UltraFocus^{DXA} (Faxitron Bioptics, Tucson, AZ) (17).

Peripheral quantitative computed tomography.

Peripheral quantitative computed tomography (pQCT) scans were performed using the peripheral quantitative computed tomography XCT Research M (v.4,5B; Norland Stratec, Pforzheim, Germany), using a voxel size of 70 μm, as previously described (18). The cortical bone parameters were analyzed in the mid-diaphyseal region of the femur, and the threshold was set to 710 mg/cm^3 (19).

High-resolution microcomputed tomography.

High-resolution microcomputed tomography (μCT) was used to analyze the distal femur and vertebra L5 (Skyscan, 1172; Bruker MicroCT, Aartselaar, Belgium), as previously described (5). Briefly, the cortical region was analyzed in the distal part of the femur, starting 5.3 mm from the growth plate and continuing 131 μm in proximal direction. The trabecular region in femur was analyzed ∼655 μm in the proximal direction from the distal growth plate and continued 131 μm in the proximal direction. For vertebra L5, the trabecular bone was analyzed 235 μm from the lower end of the pedicles and continued for ∼229 μm. The data were analyzed using the CTAn software (Bruker MicroCT).

Dynamic histomorphometry.

For the dynamic histomorphometric analyses of the mid-diaphyseal region of femur, the mice were injected intraperitoneally with the fluorochromes calcein and alizarin (Merck GmbH, Darmstadt, Germany) 9 and 2 days before they were euthanized, respectively (5). After dissection, the femurs were fixated in 4% formaldehyde and dehydrated in EtOH. The femurs were defatted in xylene and embedded in methyl methacrylate. The sections used had a thickness of 50–80 μm and were obtained from a standardized site of the femoral shaft. The analyses of dynamic cortical bone parameters were performed without staining. All parameters were analyzed using OsteoMeasure7 histomorphometry system (OsteoMetrics, Atlanta, GA)

and following the guidelines of the American Society for Bone and Mineral Research (20).

Mechanical strength.

The left humerus was frozen at −20°C directly after dissection. Three-point bending of humerus was performed with a loading speed of 0.155 mm/s and a span length of 4.5 mm, using an Instron 3366 (Instron, Norwood, MA). The biomechanical parameters were based on the recorded load deformation curves and calculated from Bluehill 2 software v2.6 (Instron) with custom-made Excel (Microsoft, Redmond, WA) macros (5).

Real-Time Quantitative PCR

Total mRNA was prepared from bone using Trizol reagent (15596018; Thermo Fischer Scientific) and RNeasy Mini Kit (74106; Qiagen). The mRNA were reversed transcribed to cDNA (4368814; Thermo Fischer Scientific), and real-time PCR analyses were performed using the StepOnePlus Real-Time PCR System (Thermo Fischer Scientific) and the following Assay-on-Demand primer and probe sets: *Notum*, Mm01253273_m1; *Alpl*, Mm00475834_m1; *Col1a1*, Mm00801666_g1; *Acp5* (encoding *TRAP*), Mm00475698_m1; *Tnfrsf11b* (encoding *OPG*), Mm00435452_m1; *Tnfsf11* (encoding *RANKL*), Mm00441908_m1; *Ctsk* (encoding *Cathepsin K*), Mm00484036_m1; *Sost* (encoding *Sclerostin*), Mm00470479_m1; *Dmp1*, Mm01208363_m1; *Wnt10b*, Mm00442104_m1; *Lef1*, Mm01310389_m1; *Tcf7* (encoding Transcription factor 1), Mm00493445_m1; *Lrp5*, Mm01227476_m1; *Lrp6*, Mm00999795_m1; *Fzd1* (encoding *Frizzled-1*), Mm00445405_s1; *Dkk1* (encoding *Dickkopf-1*), Mm00438422_m1; *Axin 2*, Mm00443610_m1; and *cMyc* Mm00487804_m1. The expressions of each gene were normalized to 18S ribosomal subunit (4310893E; Thermo Fischer Scientific). The $2^{-\Delta\Delta Ct}$ method was used to calculate the relative gene expression.

Serum Analyses

The ELISA RatLaps Kit (AC-06F1, Immunodiagnostic Systems, East Boldon, UK) was used to measure serum levels of COOH-terminal type I collagen (CTX) fragments to assess bone resorption. To assess bone formation, serum levels of procollagen type I NH_2-terminal propeptide (P1NP) were measured using a Rat/Mouse EIA Kit (AC-33F1, Immunodiagnostic Systems).

In Situ Hybridization

Femur from 5-mo-old wild-type mice were fixed in 4% formaldehyde in phosphate-buffered saline, followed by demineralization in 15% EDTA with 0.4% PFA for 3 wk. The decalcified femurs were dehydrated and processed for paraffin embedding. Six-micrometer-thick longitudinal consecutive dewaxed sections were used for in situ hybridization using RNAscope 2.5 HD Brown technology 322300 (Advanced Cell Diagnostics, Bio-Techne Ltd., Abingdon, UK). The following probes were used: *Notum* (428981, target sequence 406–1623, Advanced Cell Diagnostics) and *Dmp1* (441171, target sequence 689–1543, Advanced Cell Diagnostics). A modified RNAscope manual protocol from Advanced Cell Diagnostics was used (21). Briefly, after pretreatment, the sections were hybridized with the probes overnight at 40°C, followed by six steps of amplification according to the manufacturer's instructions. To further amplify the signal, the DAB staining step was omitted and the signal was amplified with Digoxigenin-labeled Tyramide signal amplification (NEL 748001KT, Akoya Biosciences, Marlborough, MA), detected by alkaline phosphatase-conjugated Anti-Digoxigenin Fab fragments (11093274910, Sigma-Aldrich, St Louis, MO), and visualized with Liquid Permanent Red (K0640, DAKO, Carpinteria, CA). Finally, the sections were counterstained with Mayer's hematoxylin (MHS1, Sigma-Aldrich) and mounted with Aquatex (1085620050, Sigma-Aldrich).

Statistical Analyses

All values are presented as means ± SE. The statistical differences between *Dmp1-creNotum*$^{flox/flox}$ mice and *Notum*$^{flox/flox}$ mice were calculated using a mixed model two-way ANOVA evaluating the effects of genotype and sex as well as their interaction, using GraphPad Prism version 8.3.0 for Windows. Two-tailed Student's *t* tests were used when only one sex was evaluated. A difference was considered significant when $P < 0.05$.

RESULTS

Osteocytes and Late Osteoblasts Express *Notum*

We have previously demonstrated that *Notum* expression is high in cortical bone (11, 13). To determine if *Notum* is expressed in *Dmp1*-expressing osteocytes and/or late osteoblasts in cortical bone, chromogenic in situ hybridization was performed. *Notum* mRNA was detected in *Dmp1*-expressing osteocytes and late osteoblasts (Fig. 1*A*), suggesting that *Dmp1*-expressing cells are the principal source of *Notum* in cortical bone.

Inactivation of *Notum* in *Dmp1*-Expressing Cells Leads to Increased Cortical Bone Mass and Reduced Cortical Porosity

To directly determine if *Dmp1*-expressing osteocytes and late osteoblasts are the principal source of *Notum* in cortical bone and to evaluate the skeletal effect of osteocyte/late osteoblast-derived *Notum*, we generated a conditional *Notum*-inactivated mouse model. To achieve inactivation of *Notum* specifically in osteocytes/late osteoblasts, mice with exons 2–8 of *Notum* flanked by *LoxP* sites were mated with mice expressing the Cre recombinase driven by the *Dmp1* promoter (Fig. 1*B*), hereafter called *Dmp1-creNotum*$^{flox/flox}$ mice. *Notum*$^{flox/flox}$ littermates were used as controls.

Notum mRNA levels in diaphyseal cortical bone were substantially lower in *Dmp1-creNotum*$^{flox/flox}$ mice, compared with *Notum*$^{flox/flox}$ littermates (−84.3 ± 2.1%, $P < 0.001$; Fig. 1*C*), demonstrating that the major part of *Notum* in cortical bone is derived from osteocytes/late osteoblasts. In contrast, no difference in *Notum* mRNA levels in liver was observed between *Dmp1-creNotum*$^{flox/flox}$ mice and *Notum*$^{flox/flox}$ littermates (Fig. 1*C*), confirming the specificity of the *Notum* inactivation.

The *Dmp1-creNotum*$^{flox/flox}$ mice were born according to Mendel's law of inheritance, and they appeared healthy

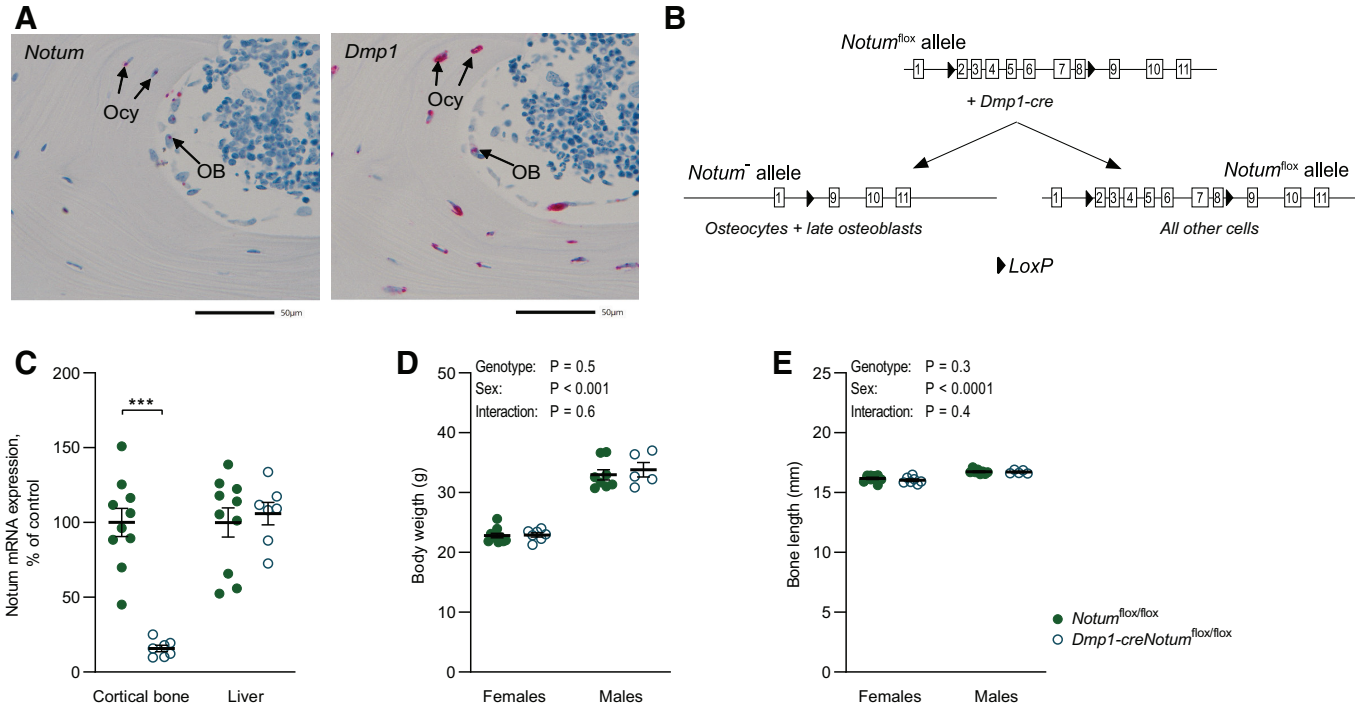

Figure 1. Normal body phenotype in mice with specific deletion of *Notum* in osteocytes/late osteoblasts. *A*: representative sections in femur of adult wild-type male mice after in situ hybridization showing *Notum* (*left*) and *Dmp1* (*right*) transcripts (labeled red) in osteocytes (Ocy) and osteoblasts (OB). *Dmp1*-labeled images (*right*) are consecutive sections of *Notum*-labeled images (*left*). Scale bar = 50 μm. *B*: schematic figure of the osteocyte and late osteoblast-specific *Notum* inactivated mouse model. *C*: mRNA expression of *Notum* in cortical bone (*left*) and liver (*right*) in *Dmp1-creNotum*$^{flox/flox}$ (n = 7) and *Notum*$^{flox/flox}$ (n = 10) female mice. *D*: normal body weight in *Dmp1-creNotum*$^{flox/flox}$ (females, n = 7; males, n = 5) and *Notum*$^{flox/flox}$ (females, n = 10; males, n = 8) mice. *E*: normal femur length in *Dmp1-creNotum*$^{flox/flox}$ (females, n = 7; males, n = 5) and *Notum*$^{flox/flox}$ (females, n = 10; males, n = 8) mice. All values are given as means ± SE. ***$P < 0.001$ compared with *Notum*$^{flox/flox}$ mice using Student's t test. A mixed model two-way ANOVA was used to assess the effects of genotype (*Dmp1-creNotum*$^{flox/flox}$ and *Notum*$^{flox/flox}$), sex, as well as their interaction. A difference was considered significant when $P < 0.05$.

compared with control littermates, with no difference in body weight (Fig. 1*D*) or femur length (Fig. 1*E*). Furthermore, the relative tissue weights of several tissues including liver, kidney, spleen, gonadal fat, retroperitoneal fat, seminal vesicles, and uterus were normal in the *Dmp1-creNotum*$^{flox/flox}$ mice (Table 1).

As we previously demonstrated that mice with inactivation of *Notum* in both early and late osteoblast-lineage cells, using *Runx2-creNotum*$^{flox/flox}$ mice (13), have increased cortical bone mass in the diaphyseal region of femur, we first performed a DXA at 12 wk of age to evaluate the phenotype of the *Dmp1-creNotum*$^{flox/flox}$ mice. We observed an increase in total body bone mineral density, when compared with *Notum*$^{flox/flox}$ mice (+5.4 ± 1.7%, P = 0.004; Supplemental Fig. S1; all Supplemental material is available at https://doi.org/10.6084/m9.figshare.13816040). After 20 wk, we screened the cortical bone parameters in the diaphyseal region of femur in *Dmp1-creNotum*$^{flox/flox}$ mice and *Notum*$^{flox/flox}$ littermates using pQCT. Two-way ANOVA analyses, evaluating both male and female mice, revealed that *Dmp1-creNotum*$^{flox/flox}$ mice displayed significantly increased cortical bone thickness (+6.1 ± 1.5%, $P < 0.001$), cortical volumetric BMD (+2.5 ± 0.6%, $P < 0.001$), and cortical bone mineral content (+9.5 ± 2.1%, $P < 0.0001$) in the

Table 1. *Tissue weights*

	Females		Males		Two-Way ANOVA		
	Notum$^{flox/flox}$	*Dmp1-creNotum*$^{flox/flox}$	*Notum*$^{flox/flox}$	*Dmp1-creNotum*$^{flox/flox}$	*P* Genotype	*P* Sex	*P* Interaction
Liver	40.1 ± 1.24	37.8 ± 2.55	41.4 ± 1.30	40.3 ± 0.99	0.3	0.3	0.5
Kidney	9.94 ± 0.32	10.1 ± 0.43	13.8 ± 0.44	14.8 ± 0.74	0.4	<0.0001	0.6
Spleen	3.50 ± 0.15	3.79 ± 0.29	3.58 ± 0.20	2.99 ± 0.17	0.5	0.1	0.05
Gonadal fat	15.8 ± 2.70	14.9 ± 2.73	16.4 ± 3.89	18.9 ± 4.64	0.8	0.5	0.6
Retroperitoneal fat	2.46 ± 0.44	2.34 ± 0.42	4.58 ± 1.22	6.79 ± 1.91	0.3	<0.001	0.3
Uterus	3.52 ± 0.60	2.49 ± 0.14					
Vesicle seminalis			9.9 ± 0.48	9.6 ± 0.26			

Values are given as means ± SE (*Notum*$^{flox/flox}$: females n = 10, males n = 8; *Dmp1-creNotum*$^{flox/flox}$: females n = 7, males n = 5, 20-wk-old mice) in mg/g body wt. A mixed model two-way ANOVA was used to evaluate the effect of genotype, sex, and their interaction. Two-tailed Student's t tests were used when only one sex was evaluated. A difference was considered significant when $P < 0.05$.

diaphyseal region of femur compared with *Notum*$^{flox/flox}$ littermates, with no significant sex interaction for any of these effects on cortical bone (Fig. 2, *A*–*D*). Analyses of the periosteal and endocortical circumferences in *Dmp1-creNotum*$^{flox/flox}$ mice did not reveal any significant effects (Fig. 2, *D* and *E*). However, a nonsignificant tendency of increased periosteal circumference (+1.1 ± 1.1%, $P = 0.2$) was observed in *Dmp1-creNotum*$^{flox/flox}$ mice compared with *Notum*$^{flox/flox}$ mice.

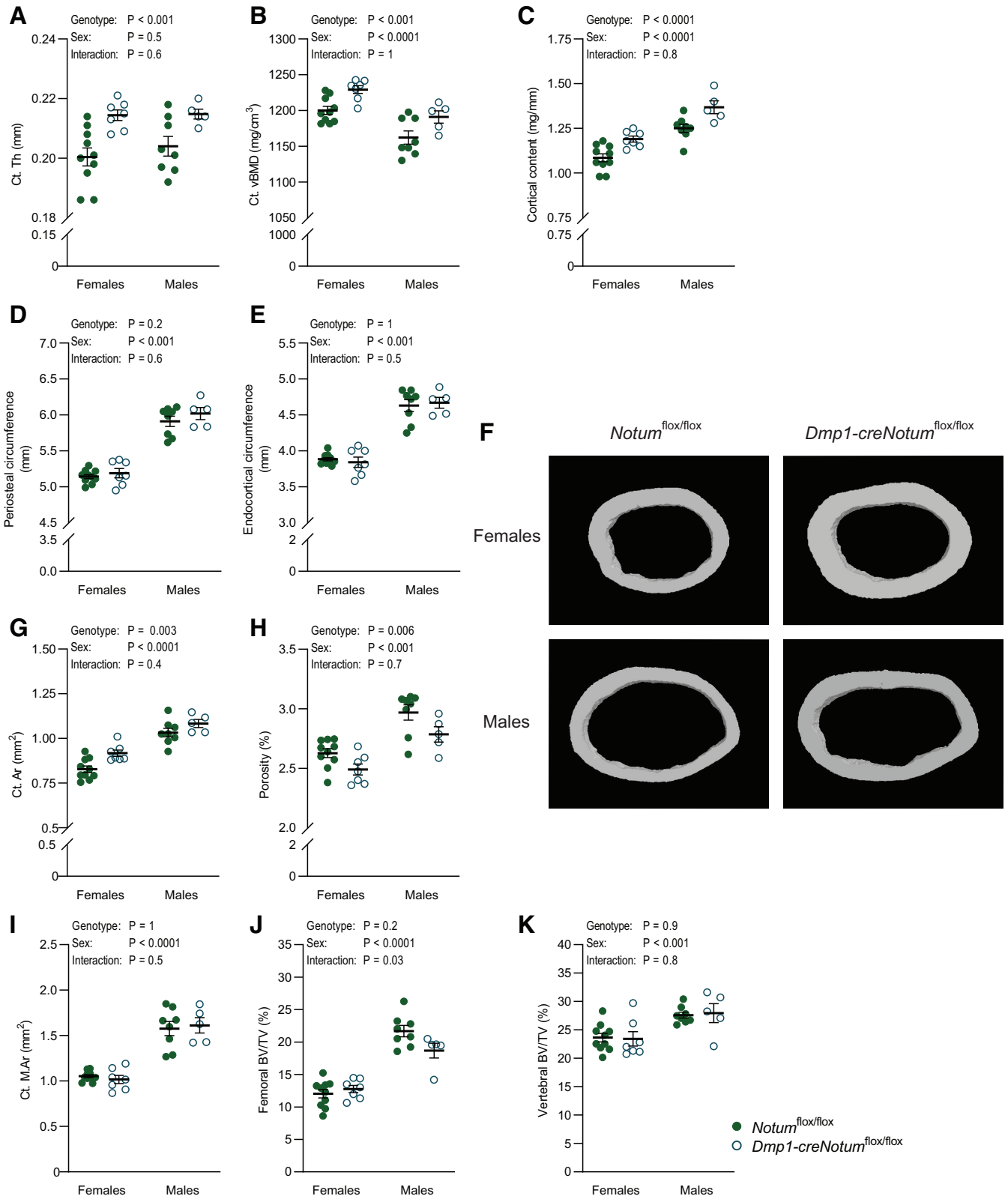

Table 2. *Dynamic histomorphometric parameters in the diaphyseal region of femur in Dmp1-creNotum$^{flox/flox}$ mice*

	Females		Males		Two-Way ANOVA		
	Notum$^{flox/flox}$	*Dmp1-creNotum*$^{flox/flox}$	*Notum*$^{flox/flox}$	*Dmp1-creNotum*$^{flox/flox}$	*P* Genotype	*P* Sex	*P* Interaction
Cortical bone width (Ct. Wi), μm	202 ± 3.90	213 ± 2.55	208 ± 4.87	222 ± 4.61	0.005	0.1	0.8
Periosteal dynamic histomorphometry							
Mineralizing surface/bone surface (MS/BS), %	56.5 ± 2.04	57.2 ± 3.02	43.3 ± 2.77	38.6 ± 4.73	0.5	<0.0001	0.4
Mineral apposition rate (MAR), μm/day	0.99 ± 0.04	0.97 ± 0.05	1.00 ± 0.05	0.83 ± 0.05	0.05	0.2	0.2
Bone formation rate/bone surface (BFR/BS), $\mu m^3/\mu m^2/yr$	205 ± 11.7	202 ± 17.2	160 ± 15.4	119 ± 18.3	0.2	<0.001	0.2
Endocortical dynamic histomorphometry							
Mineralizing surface/bone surface (MS/BS), %	62.7 ± 2.84	56.3 ± 4.07	33.6 ± 3.1	34.5 ± 1.10	0.4	<0.0001	0.3
Mineral apposition rate (MAR), μm/day	1.02 ± 0.06	0.98 ± 0.09	0.84 ± 0.11	0.98 ± 0.17	0.6	0.4	0.4
Bone formation rate/bone surface (BFR/BS), $\mu m^3/\mu m^2/yr$	238 ± 21.2	205 ± 29.1	105 ± 16.6	121 ± 18.1	0.7	<0.0001	0.3

Values are given as means ± SE (*Notum*$^{flox/flox}$: females $n = 10$, males $n = 8$; *Dmp1-creNotum*$^{flox/flox}$: females $n = 7$, males $n = 5$, 20-wk-old mice). A mixed model two-way ANOVA was used to evaluate the effect of genotype, sex, and their interaction. A difference was considered significant when $P < 0.05$.

The increased cortical bone mass in *Dmp1-creNotum*$^{flox/flox}$ mice was confirmed by μCT (Fig. 2*F*), revealing increased cortical bone area (+7.6 ± 2.3%, $P = 0.003$) in the femur diaphysis compared with *Notum*$^{flox/flox}$ littermates (Fig. 2*G*). μCT analysis also revealed lower cortical porosity (−5.7 ± 1.9%, $P = 0.006$) in *Dmp1-creNotum*$^{flox/flox}$ mice compared with *Notum*$^{flox/flox}$ littermates, indicating that inactivation of *Notum* results not only in increased cortical bone mass but also in a higher quality of the cortical bone (Fig. 2*H*). No significant sex interaction was observed for the effect of *Notum* inactivation on cortical bone area or on cortical porosity (Fig. 2, *G* and *H*). The cross-sectional bone marrow area was not affected in *Dmp1-creNotum*$^{flox/flox}$ mice compared with *Notum*$^{flox/flox}$ littermates (Fig. 2*I*). The increased amount of cortical bone in the diaphyseal region of femur in *Dmp1-creNotum*$^{flox/flox}$ mice was also confirmed by histomorphometry analyses (Table 2). In contrast to the clear effects on cortical bone parameters, *Dmp1-creNotum*$^{flox/flox}$ mice had unchanged trabecular bone volume fraction in the distal metaphyseal region of femur and in the lumbar vertebra L5 as measured using μCT (Fig. 2, *J* and *K*). Thus, similar to the mice with inactivation of *Notum* in both early and late osteoblast-lineage cells, using *Runx2-creNotum*$^{flox/flox}$ mice (13), *Notum* inactivation specifically in osteocytes/late osteoblasts, using *Dmp1-creNotum*$^{flox/flox}$ mice, results in increased cortical bone mass without any effect on trabecular bone volume fraction.

Three-point bending analyses of the mechanical strength of humerus revealed a nonsignificant tendency of increased maximal load at failure (+7.7 ± 5.0%, $P = 0.1$) in *Dmp1-creNotum*$^{flox/flox}$ mice compared with *Notum*$^{flox/flox}$ mice while no effect was observed on toughness or stiffness (Table 3).

A New Steady State of Bone Turnover in the Adult *Dmp1-creNotum*$^{flox/flox}$ Mice

We have previously demonstrated that an acute inducible *Notum* inactivation in adulthood results in an increased cortical bone thickness via a rapid increase in cortical bone formation, while the increased cortical bone thickness in adult *Runx2-creNotum*$^{flox/flox}$ mice with lifelong *Notum* inactivation is not associated with a sustained adult increased bone formation, most likely as a new steady state of bone turnover has been reached (13). To determine if the increased cortical bone mass in the *Dmp1-creNotum*$^{flox/flox}$ mice with lifelong *Notum* inactivation in osteocytes/late osteoblasts is associated with an increased cortical bone formation in adulthood, dynamic histomorphometry was performed in the mid-diaphyseal cortical region of femur in 20-wk-old mice. Neither the periosteal nor the endocortical bone formation rate was affected in the adult *Dmp1-*

Figure 2. Bone characteristics in mice with conditional *Notum* inactivation in osteocytes and late osteoblasts. *A*–*C*: cortical thickness (Ct. Th; *A*), cortical density (Ct. vBMD; *B*), and cortical content (*C*) of femur measured by peripheral quantitative computed tomography (pQCT) in *Dmp1-creNotum*$^{flox/flox}$ (females, $n = 7$; males, $n = 5$) mice and *Notum*$^{flox/flox}$ (females, $n = 10$; males, $n = 8$) mice. *D* and *E*: periosteal circumference (*D*) and endocortical circumference (*E*) of the femur, measured by pQCT in *Dmp1-creNotum*$^{flox/flox}$ (females, $n = 7$; males, $n = 5$) mice and *Notum*$^{flox/flox}$ (females, $n = 10$; males, $n = 8$) mice. *F*–*I*: representative 3-dimensional images of cortical bone (*F*), cross-sectional cortical area (Ct. Ar; *G*), cortical porosity (*H*), and cross-sectional marrow area (Ct. M. Ar; *I*) of the femur, measured by microcomputed tomography (μCT) in *Dmp1-creNotum*$^{flox/flox}$ (females, $n = 7$; males, $n = 5$) mice and *Notum*$^{flox/flox}$ (females, $n = 10$; males, $n = 8$) mice. *J* and *K*: trabecular bone volume over tissue volume (BV/TV) in femur (*J*) and vertebra L5 (*K*), measured by μCT in *Dmp1-creNotum*$^{flox/flox}$ (females, $n = 7$; males, $n = 5$) mice and *Notum*$^{flox/flox}$ (females, $n = 10$; males, $n = 8$) mice. The results refer to 20-wk-old mice. All values are given as means ± SE. A mixed model two-way ANOVA was used to assess the effects of genotype (*Dmp1-creNotum*$^{flox/flox}$ and *Notum*$^{flox/flox}$), sex, as well as their interaction. A difference was considered significant when $P < 0.05$.

Table 3. *Biomechanical parameters from three-point bending of the humerus*

	Females		Males		Two-Way ANOVA		
	Notum$^{flox/flox}$	*Dmp1-creNotum*$^{flox/flox}$	*Notum*$^{flox/flox}$	*Dmp1-creNotum*^{floxFlox}	*P* Genotype	*P* Sex	*P* Interaction
Maximal load, N	14.7 ± 0.60	16.5 ± 0.73	18.5 ± 0.66	19.2 ± 0.55	0.1	<0.0001	0.4
Toughness, mJ	4.78 ± 0.51	6.02 ± 0.35	6.10 ± 0.73	5.81 ± 0.57	0.4	0.4	0.2
Stiffness, N/mm	110 ± 9.04	127 ± 8.85	143 ± 11.8	113 ± 13.9	0.5	0.4	0.04

Values are given as means ± SE (*Notum*$^{flox/flox}$: females n = 10, males n = 8; *Dmp1-creNotum*$^{flox/flox}$: females n = 7, males n = 5, 20-wk-old mice). A mixed model two-way ANOVA was used to evaluate the effect of genotype, sex, and their interaction. A difference was considered significant when $P < 0.05$.

creNotum$^{flox/flox}$ mice compared with *Notum*$^{flox/flox}$ mice (Table 2). Furthermore, gene expression analyses of cortical bone revealed unchanged mRNA levels both of genes reflecting bone formation and of genes reflecting bone resorption (Supplemental Table S1). Analyzes of the expression of osteocyte and WNT signaling genes showed no differences in mRNA levels between *Dmp1-creNotum*$^{flox/flox}$ and *Notum*$^{flox/flox}$ mice (Supplemental Table S1). In addition, no significant effect of lifelong *Notum* inactivation in *Dmp1-creNotum*$^{flox/flox}$ mice was observed on the adult serum levels of the bone resorption marker COOH-terminal telopeptide (CTX) or the bone formation marker Procollagen type I NH_2-terminal propeptide (P1NP; Supplemental Table S2). These results indicate that a new steady state of bone remodeling has been reached in the adult *Dmp1-creNotum*$^{flox/flox}$ mice with lifelong inactivation of *Notum* in osteocytes/late osteoblasts.

DISCUSSION

Cortical bone is a major determinant of fracture risk at nonvertebral bone sites, but the knowledge of the mechanisms for regulation of cortical bone mass is limited (22). We have previously demonstrated that the WNT lipase NOTUM is a major regulator of cortical bone mass (11, 13). However, the exact origin of NOTUM with an impact on cortical bone was unknown. We, herein, demonstrate *Notum* expression in *Dmp1*-expressing osteocytes/late osteoblasts in cortical bone. Furthermore, in functional studies we demonstrate that *Dmp1*-expressing osteocytes/late osteoblasts are the principal source of *Notum* in cortical bone and that *Notum* derived from osteocytes/late osteoblasts reduces cortical bone mass. There is medical need for new safe treatment strategies that increase cortical bone mass and thereby reduce nonvertebral fracture risk. The present findings, together with our recent reports (11, 13), indicate that NOTUM inhibition may be a promising drug target to increase cortical bone mass and reduce nonvertebral fracture risk.

We have previously demonstrated that *Notum* is highly expressed in cortical bone and that relatively high *Notum* expression is observed in cultured osteoblasts but not osteoclasts (11, 13). In the present study, we extended those findings by showing that *Notum* is expressed in *Dmp1*-expresssing osteocytes/late osteoblasts using the in situ hybridization technique RNAscope. We, therefore, hypothesized that osteocytes/late osteoblasts are the principal source of NOTUM with an impact on cortical bone. To directly determine if *Dmp1*-expressing osteocytes and late osteoblasts are the principal source of NOTUM in cortical bone and to evaluate the skeletal effect of osteocytes/late osteoblasts-derived NOTUM, we generated a conditional *Notum*-inactivated mouse model. We observed that the *Dmp1-creNotum*$^{flox/flox}$ mice displayed a substantial reduction of *Notum* mRNA in cortical bone, demonstrating that the major part of NOTUM in cortical bone is indeed derived from osteocytes/late osteoblasts. In contrast, no difference in *Notum* mRNA levels was observed in the liver, confirming the specificity of the *Notum* inactivation in the *Dmp1-creNotum*$^{flox/flox}$ mouse model.

The *Dmp1-creNotum*$^{flox/flox}$ mice appeared healthy, with no difference in body weight or femur length, demonstrating that the observed increased cortical bone mass is specific and not only the result of an increased overall growth of the mice. This finding correlates with our previous finding using mice with inactivation of *Notum* in both early and late osteoblast-lineage cells, using *Runx2-creNotum*$^{flox/flox}$ mice that also had increased cortical bone mass but normal overall body size (13).

The reduction of *Notum* mRNA in cortical bone and the skeletal phenotype observed in the *Dmp1-creNotum*$^{flox/flox}$ mice, including increased cortical bone mass but unchanged trabecular bone mass, are identical to what we have previously reported for mice with lifelong inactivation of *Notum* in both early and late osteoblast lineage cells and mice with global inducible inactivation of *Notum* in adulthood (13). When comparing the effects of *Notum* inactivation in the *Dmp1-creNotum*$^{flox/flox}$ mice, in the present study, and the effects of *Notum* inactivation in the *Runx2-creNotum*$^{flox/flox}$ mice from our previous report (13), we observed that *Notum* mRNA in cortical bone was substantially reduced (*Dmp1-creNotum*$^{flox/flox}$ mice: −77.6 ± 9.3%; *Runx2-creNotum*$^{flox/flox}$ mice: −87.9 ± 11.4%) while cortical bone area was significantly increased (*Dmp1-creNotum*$^{flox/flox}$ mice: +7.6 ± 2.3%; *Runx2-creNotum*$^{flox/flox}$ mice: +13.5 ± 2.5%) in both mouse models (13). In addition, the trabecular bone volume fraction in the vertebra or femur was not significantly affected in any of the two mouse models (13). Thus the two mouse models display a similar specific cortical bone phenotype, strongly suggesting that NOTUM in osteocytes/late osteoblasts but not in osteoblast precursors/early osteoblasts is crucial for the physiological effect of NOTUM on cortical bone.

These functional data demonstrate that NOTUM derived from osteocytes/late osteoblasts reduces cortical bone mass. Deletion of β-catenin in osteocytes has been reported to reduce bone mass in mice, demonstrating that WNT/β-catenin signaling in osteocytes is needed for normal bone homeostasis (23). It is, therefore, possible that NOTUM inhibits β-catenin-dependent WNT signaling in osteocytes of cortical bone.

As the inactivation of *Notum* in the *Dmp1-creNotum*$^{flox/flox}$ mice is lifelong, one may argue that the observed effects on the skeleton may be the result of early developmental effects in this mouse model. However, the identical cortical bone phenotype observed in our previous study using global inducible *Notum* inactivation in adulthood strongly argues against major confounding developmental effects in the *Dmp1-creNotum*$^{flox/flox}$ mice (13).

We have previously demonstrated that an acute inducible *Notum* inactivation in adulthood results in an increased cortical bone thickness via a rapid increase in adult cortical bone formation while the increased cortical bone thickness in the adult *Runx2-creNotum*$^{flox/flox}$ mice with lifelong *Notum* inactivation is not associated with a sustained adult increased bone formation, most likely as a new steady state of bone turnover had been reached (13). Consistent with these previous findings, the increased cortical bone mass in the adult *Dmp1-creNotum*$^{flox/flox}$ mice with lifelong *Notum* inactivation in osteocytes/late osteoblasts in the present study was not associated with any significant changes in parameters reflecting bone formation, bone resorption, or WNT signaling, indicating that a new steady state of bone remodeling has been reached in the adult *Dmp1-creNotum*$^{flox/flox}$ mice.

A limitation of the present study is the lack of further cellular and molecular mechanisms by which NOTUM exerts its effect besides those which we have previously reported (13).

Another limitation of the present study is the relative low numbers of mice, resulting in low power in some of the analyses, including the bone strength measurements using three-point bending.

In conclusion, *Dmp1*-expressing osteocytes/late osteoblasts are the principal source of NOTUM in cortical bone and NOTUM derived from osteocytes/late osteoblasts reduces cortical bone mass. These findings support the concept that inhibition of osteocytes/late osteoblasts-derived NOTUM might be an interesting pharmacological target to increase cortical bone mass and reduce nonvertebral fracture risk.

ACKNOWLEDGMENTS

The authors thank Anna Westerlund and Ulrika Björklund from the University of Gothenburg for excellent technical assistance.

Present address of M. El Shahawy: Dept. of Oral Biology, Minia University, Minia, Egypt.

GRANTS

This study was supported by the Swedish Research Council, the Swedish Foundation for Strategic Research, the Swedish state under the agreement between the Swedish government and the county councils, the ALF-agreement in Gothenburg (Grants 238261, 226481, and 237551), the IngaBritt and Arne Lundberg Foundation, the Royal 80 Year Fund of King Gustav V, the Torsten and Ragnar Söderberg's Foundation, the Knut and Alice Wallenberg Foundation, the Novo Nordisk Foundation, and the Adlerbertska Research Foundation.

DISCLOSURES

No conflicts of interest, financial or otherwise, are declared by the authors.

AUTHOR CONTRIBUTIONS

U.H.L., C.O., and S.M.-S. conceived and designed research; K.H.N., P.H., M.E.S., J.W., A.K., J.T., and S.M.-S. performed experiments; K.H.N., P.H., S.M.-S. analyzed data; K.H.N., P.H., U.H.L., C.O., and S.M.-S. interpreted results of experiments; K.H.N. prepared figures; K.H.N. drafted manuscript; K.H.N., P.H., M.E.S., J.W., A.K., J.T., C.P., U.H.L., C.O., and S.M.-S. edited and revised manuscript; K.H.N., C.O., and S.M.-S. approved final version of manuscript.

REFERENCES

1. **Baron R**, **Hesse E.** Update on bone anabolics in osteoporosis treatment: rationale, current status, and perspectives. *J Clin Endocrinol Metab* 97: 311–325, 2012. doi:10.1210/jc.2011-2332.
2. **Johnell O**, **Kanis J.** Epidemiology of osteoporotic fractures. *Osteoporosis Intl* 16, Suppl 2: S3–7, 2005. doi:10.1007/s00198-004-1702-6.
3. **Borgström F**, **Karlsson L**, **Ortsäter G**, **Norton N**, **Halbout P**, **Cooper C**, **Lorentzon M**, **McCloskey EV**, **Harvey NC**, **Javaid MK**, **Kanis JA**, **International Osteoporosis Foundation.** Fragility fractures in Europe: burden, management and opportunities. *Arch Osteoporos* 15: 59, 2020. doi:10.1007/s11657-020-0706-y.
4. **Hernlund E**, **Svedbom A**, **Ivergård M**, **Compston J**, **Cooper C**, **Stenmark J**, **McCloskey EV**, **Jönsson B**, **Kanis JA.** Osteoporosis in the European Union: medical management, epidemiology and economic burden. A report prepared in collaboration with the International Osteoporosis Foundation (IOF) and the European Federation of Pharmaceutical Industry Associations (EFPIA). *Arch Osteoporosis* 8: 136, 2013. doi:10.1007/s11657-013-0136-1.
5. **Moverare-Skrtic S**, **Henning P**, **Liu X**, **Nagano K**, **Saito H**, **Borjesson AE**, **Sjogren K**, et al**.** Osteoblast-derived WNT16 represses osteoclastogenesis and prevents cortical bone fragility fractures. *Nat Med* 20: 1279–1288, 2014. doi:10.1038/nm.3654.
6. **Lerner UH**, **Ohlsson C.** The WNT system: background and its role in bone. *J Intern Med* 277: 630–649, 2015. doi:10.1111/joim.12368.
7. **Ohlsson C**, **Sundh D**, **Wallerek A**, **Nilsson M**, **Karlsson M**, **Johansson H**, **Mellstrom D**, **Lorentzon M.** Cortical bone area predicts incident fractures independently of areal bone mineral density in older men. *J Clin Endocrinol Metab* 102: 516–552, 2017. doi:10.1210/jc.2016-3177.
8. **Zhong Z**, **Zylstra-Diegel CR**, **Schumacher CA**, **Baker JJ**, **Carpenter AC**, **Rao S**, **Yao W**, **Guan M**, **Helms JA**, **Lane NE**, **Lang RA**, **Williams BO.** Wntless functions in mature osteoblasts to regulate bone mass. *Proc Natl Acad Sci U S A* 109: E2197–2204, 2012. doi:10.1073/pnas.1120407109.
9. **Bennett CN**, **Longo KA**, **Wright WS**, **Suva LJ**, **Lane TF**, **Hankenson KD**, **MacDougald OA.** Regulation of osteoblastogenesis and bone mass by Wnt10b. *Proc Natl Acad Sci U S A* 102: 3324–3329, 2005. doi:10.1073/pnas.0408742102.
10. **Stevens JR**, **Miranda-Carboni GA**, **Singer MA**, **Brugger SM**, **Lyons KM**, **Lane TF.** Wnt10b deficiency results in age-dependent loss of bone mass and progressive reduction of mesenchymal progenitor cells. *J Bone Miner Res* 25: 2138–2147, 2010. doi:10.1002/jbmr.118.
11. **Brommage R**, **Liu J**, **Vogel P**, **Mseeh F**, **Thompson AY**, **Potter DG**, **Shadoan MK**, **Hansen GM**, **Jeter-Jones S**, **Cui J**, **Bright D**, **Bardenhagen JP**, **Doree DD**, **Moverare-Skrtic S**, **Nilsson KH**, **Henning P**, **Lerner UH**, **Ohlsson C**, **Sands AT**, **Tarver JE**, **Powell DR**, **Zambrowicz B**, **Liu Q.** NOTUM inhibition increases endocortical bone formation and bone strength. *Bone Res* 7: 2, 2019. doi:10.1038/s41413-018-0038-3.
12. **Kakugawa S**, **Langton PF**, **Zebisch M**, **Howell SA**, **Chang TH**, **Liu Y**, **Feizi T**, **Bineva G**, **O'Reilly N**, **Snijders AP**, **Jones EY**, **Vincent JP.** Notum deacylates Wnt proteins to suppress signalling activity. *Nature* 519: 187–192, 2015. doi:10.1038/nature14259.
13. **Moverare-Skrtic S**, **Nilsson KH**, **Henning P**, **Funck-Brentano T**, **Nethander M**, **Rivadeneira F**, **Coletto Nunes G**, **Koskela A**, **Tuukkanen J**, **Tuckermann J**, **Perret C**, **Souza PPC**, **Lerner UH**, **Ohlsson C.** Osteoblast-derived NOTUM reduces cortical bone mass in mice and the NOTUM locus is associated with bone mineral density in humans. *FASEB J* 33: 11163–11179, 2019. doi:10.1096/fj.201900707R.

14. **Nusse R.** Cell signalling: disarming Wnt. *Nature* 519: 163–164, 2015. doi:10.1038/nature14208.
15. **Canal F**, **Charawi S**, **Grimber G**, **Houbron C**, **Drouet V**, **Colnot S**, **Terris B**, **Cavard C**, **Perret C.** Generation of mice with hepatocyte-specific conditional deletion of Notum. *PLoS One* 11: e0150997, 2016. doi:10.1371/journal.pone.0150997.
16. **Lu Y**, **Xie Y**, **Zhang S**, **Dusevich V**, **Bonewald LF**, **Feng JQ.** DMP1-targeted Cre expression in odontoblasts and osteocytes. *J Dent Res* 86: 320–325, 2007. doi:10.1177/154405910708600404.
17. **Quarta C**, **Clemmensen C**, **Zhu Z**, **Yang B**, **Joseph SS**, **Lutter D**, et al**.** Molecular integration of incretin and glucocorticoid action reverses immunometabolic dysfunction and obesity. *Cell Metab* 26: 620–632e626, 2017. doi:10.1016/j.cmet.2017.08.023.
18. **Windahl SH**, **Vidal O**, **Andersson G**, **Gustafsson JA**, **Ohlsson C.** Increased cortical bone mineral content but unchanged trabecular bone mineral density in female ERbeta(-/-) mice. *J Clin Invest* 104: 895–901, 1999. doi:10.1172/JCI6730.
19. **Vidal O**, **Lindberg MK**, **Hollberg K**, **Baylink DJ**, **Andersson G**, **Lubahn DB**, **Mohan S**, **Gustafsson JA**, **Ohlsson C.** Estrogen receptor specificity in the regulation of skeletal growth and maturation in male mice. *Proc Natl Acad Sci U S A* 97: 5474–5479, 2000. doi:10.1073/pnas.97.10.5474.
20. **Dempster DW**, **Compston JE**, **Drezner MK**, **Glorieux FH**, **Kanis JA**, **Malluche H**, **Meunier PJ**, **Ott SM**, **Recker RR**, **Parfitt AM.** Standardized nomenclature, symbols, and units for bone histomorphometry: a 2012 update of the report of the ASBMR Histomorphometry Nomenclature Committee. *J Bone Miner Res* 28: 2–17, 2013. doi:10.1002/jbmr.1805.
21. **Lassen NE**, **Andersen TL**, **Pløen GG**, **Søe K**, **Hauge EM**, **Harving S**, **Eschen GET**, **Delaisse JM.** Coupling of bone resorption and formation in real time: new knowledge gained from human haversian BMUs. *J Bone Miner Res* 32: 1395–1405, 2017. doi:10.1002/jbmr.3091.
22. **Brommage R**, **Ohlsson C.** Translational studies provide insights for the etiology and treatment of cortical bone osteoporosis. *Best Pract Res Clin Endocrinol Metab* 32: 329–340, 2018. doi:10.1016/j.beem.2018.02.006.
23. **Kramer I**, **Halleux C**, **Keller H**, **Pegurri M**, **Gooi JH**, **Weber PB**, **Feng JQ**, **Bonewald LF**, **Kneissel M.** Osteocyte Wnt/beta-catenin signaling is required for normal bone homeostasis. *Mol Cell Biol* 30: 3071–3085, 2010. doi:10.1128/MCB.01428-09.